Supporting Information

Sullivan and Holyoak 10.1073/pnas.0805364105

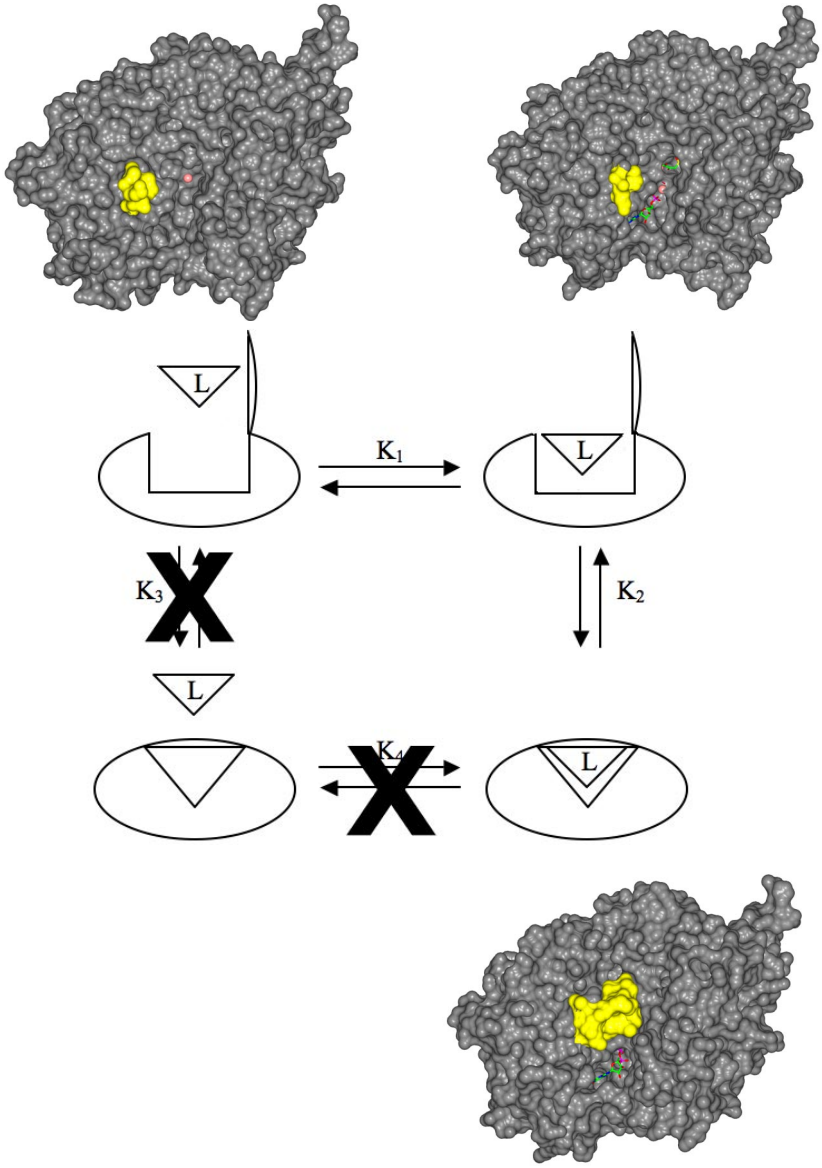

Fig. S1. Cartoon diagram of the thermodynamic cycle for the formation of the active key–lock state in the PEPCK-catalyzed reaction. The induced fit pathway is represented by the equilibrium constants K_1 and K_2 whereas the conformational selection pathway is represented by the equilibrium constants K_3 and K_4. The structures of the PEPCK–Mn^{2+}, PEPCK–Mn^{2+}–β-SP–Mn^{2+}GTP (open), and PEPCK–Mn^{2+}–β-SP–Mn^{2+}GTP (closed) complexes are positioned adjacent to the state that they mimic in the scheme (clockwise, left to right). In these structures the molecule is rendered as a gray space-filling model, while the active site lid domain is rendered in yellow. The location of the active site is indicated by the manganese ion(s) (pink sphere(s)) and the stick models of the bound ligands. As shown, the conformational selection pathway is not possible due to steric occlusion of the active site by the closure of the lid domain.

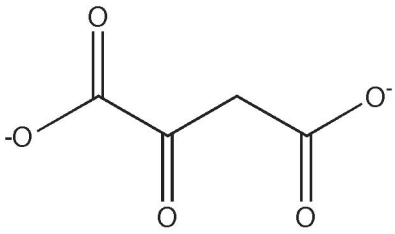

oxaloacetate

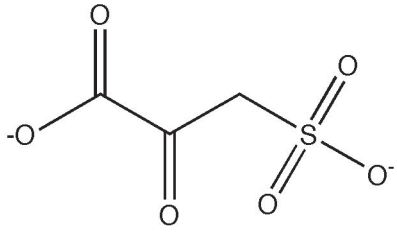

β-sulfopyruvate

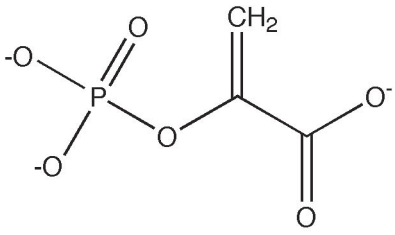

PEP

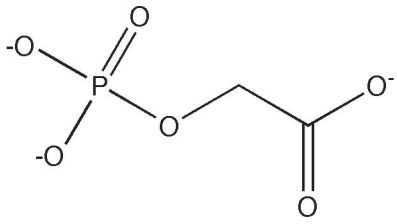

PGA

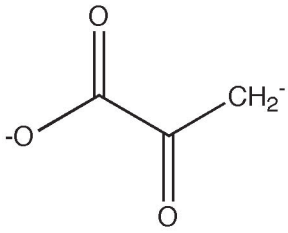

enolate of pyruvate

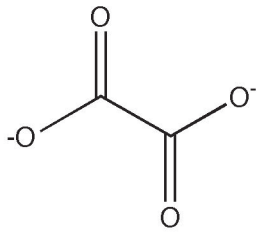

oxalate

Fig. S2. A comparison of the structures of substrate/intermediate analogues used in the structural studies with the compounds that they mimic in the PEPCK-catalyzed reaction.

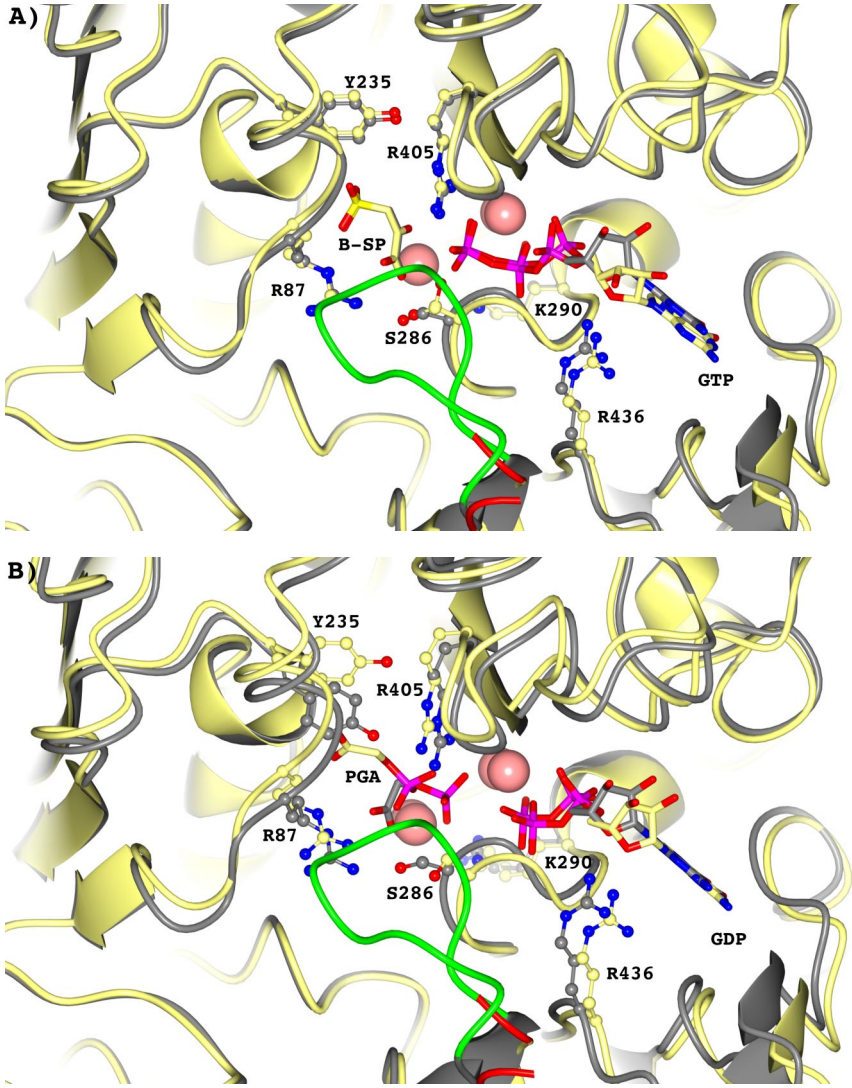

Fig. S3. Superimposing of the open- and closed-lid conformations of the (*A*) β-SP–GTP and (*B*) PGA–GDP complexes. The structure of the open-lid conformation is rendered in lemon, whereas the closed-lid structure is rendered in gray. The lid domains (463–474) are rendered in green and red in the closed and open conformations, respectively.

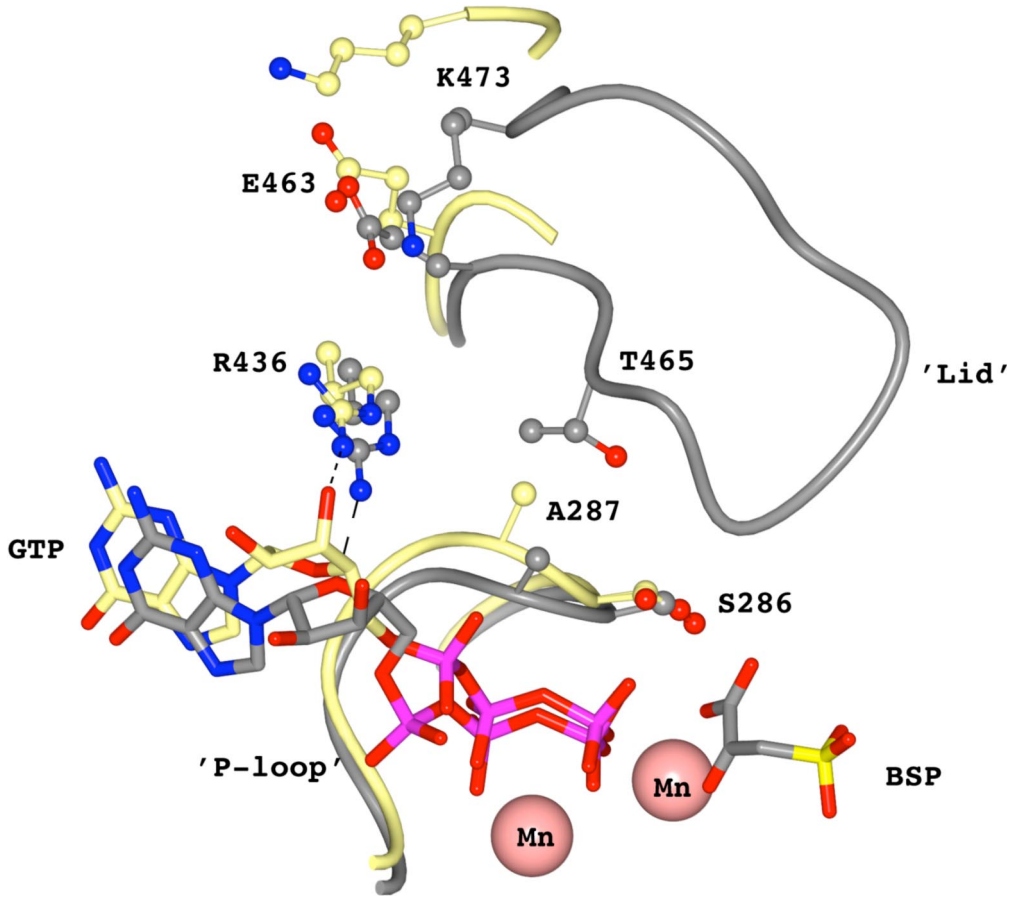

Fig. S4. Superposing of the open- and closed-lid conformations of the β-SP–GTP complex illustrating the potential steric clash between A287 of the P-loop and T465 of the lid domain if the P-loop occupies any conformation other than the fully closed one. The structure of the open conformation is rendered in lemon, whereas the closed conformation is rendered in gray. The active site and nucleotide metals are shown as pink spheres.

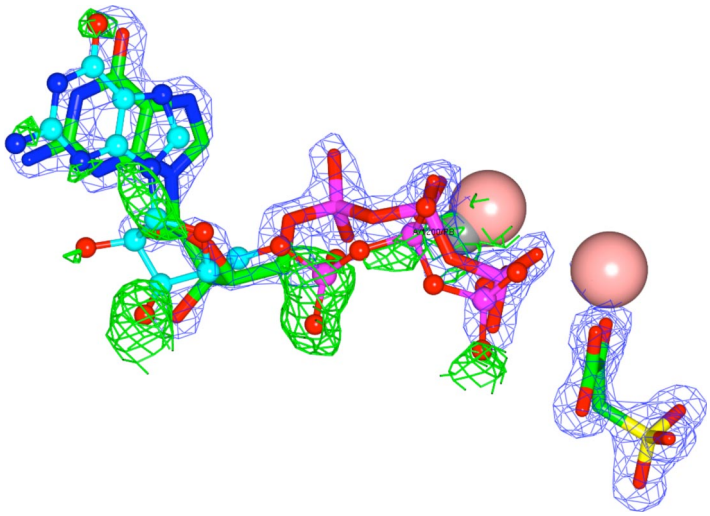

Fig. S5. Evidence for the presence of a minor occupancy of the open-lid conformation of the GTP nucleotide in the closed-lid molecule of the β-SP–GTP complex. $2F_o - F_c$ density for the major nucleotide conformation rendered at 2σ is shown as a blue mesh. The $F_o - F_c$ density after refinement of the major conformation rendered at 2σ is shown as a green mesh. The major conformation of the GTP nucleotide is rendered as a green stick model colored by atom type. The minor conformation is shown as a blue ball-and-stick model also colored by atom type. The active site and nucleotide-associated manganese ions are rendered as pink spheres, whereas the nucleotide-associated metal for the minor conformation is rendered at 0.5 of the van der Waals radius as a gray sphere.

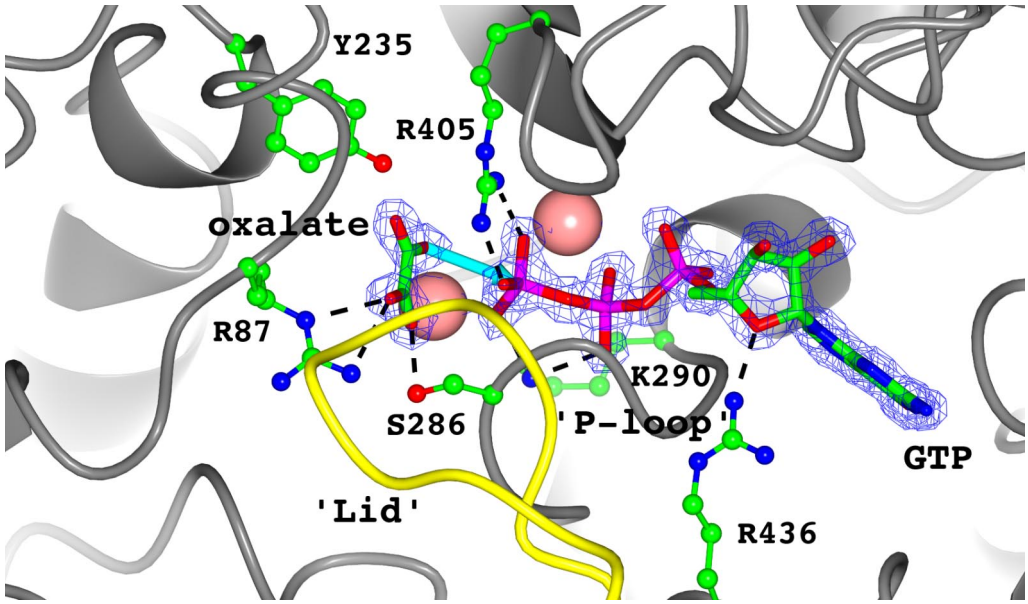

Fig. S6. The active site of the PEPCK–Mn^{2+}–oxalate–Mn^{2+}GTP complex possesses a closed-lid domain. Catalytic residues discussed in the text are rendered as ball-and-stick models whereas the oxalate and GTP ligands are rendered as thick sticks. Potential hydrogen bonds and ionic interactions between the ligands and the active site residues are indicated with dashed lines. The protein backbone is rendered as a gray ribbon except for the region corresponding to the active site lid domain (463–474) that is colored yellow. The active site and nucleotide-associated metals are rendered as pink spheres at 0.8 of their van der Waals radius. $2F_o - F_c$ density rendered at 2σ is shown for oxalate and GTP as a blue mesh. The P-loop motif containing S286 and K290 is also labeled. A thick blue arrow indicates the potential phosphoryl transfer distance between the two ligands. The potential phosphoryl transfer distance between the two ligands is 3.2 Å.

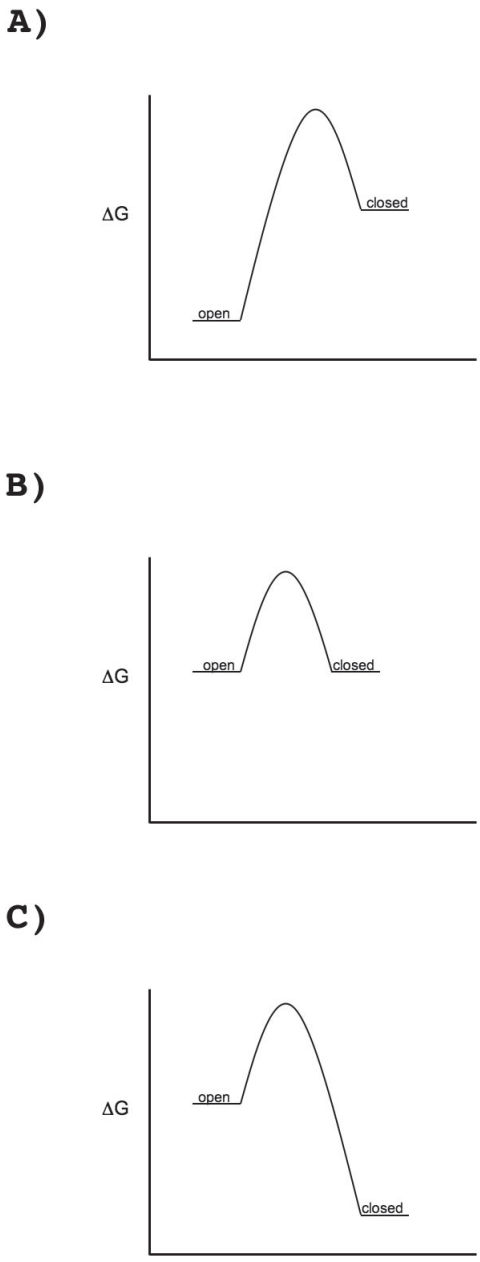

Fig. S7. A cartoon version of the energy diagrams for the conformational transition between the lid open and closed states in the holoenzyme (*A*), Michaelis (*B*), and enolate intermediate (*C*) complexes.

Scheme 1: The PEPCK reaction mechanism.

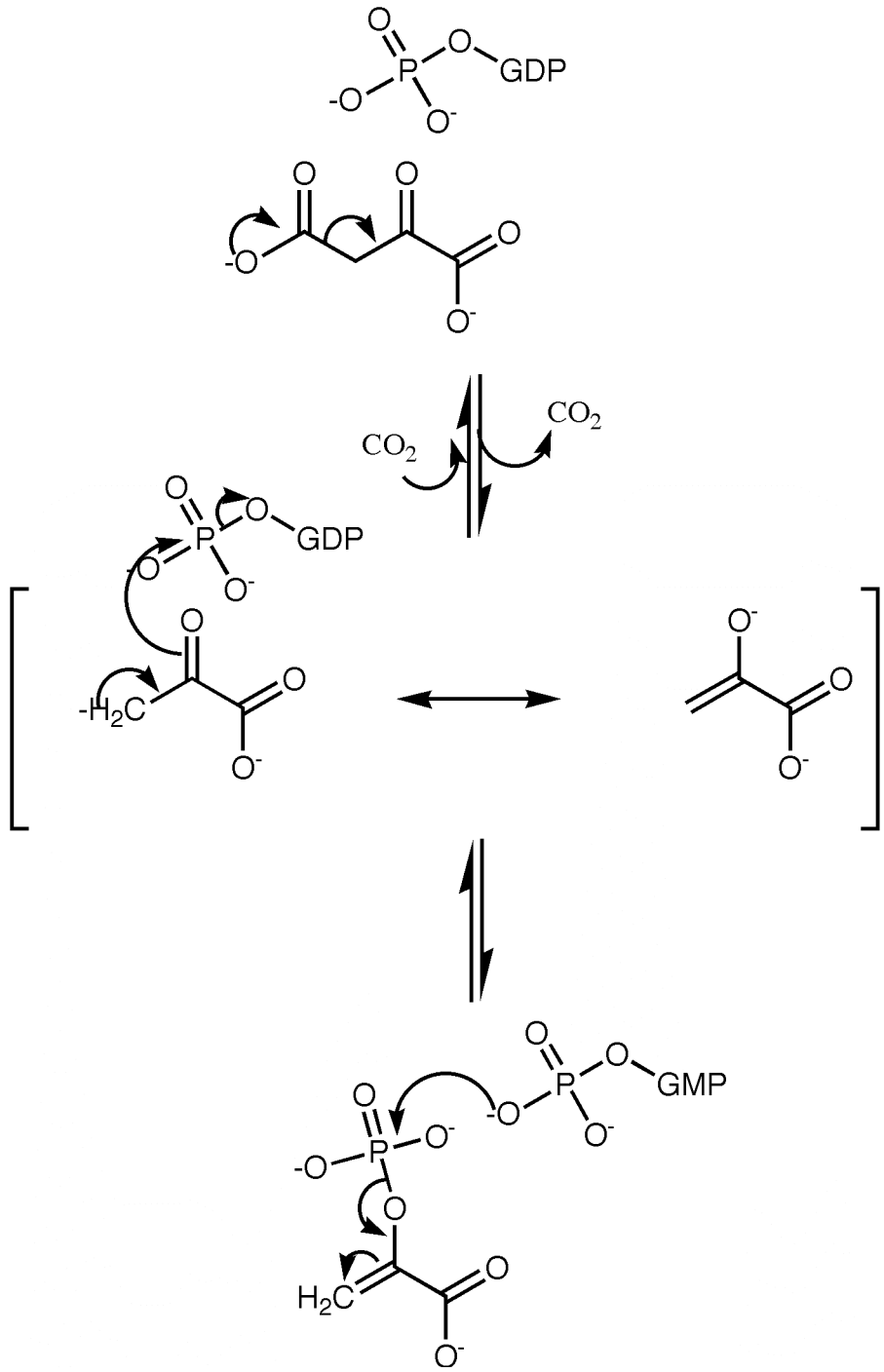

Scheme S1. The PEPCK reaction mechanism.

Table S1. Data and model statistics for the PEPCK–Mn^{2+}–β-SP–Mn^{2+}GTP, PEPCK–Mn^{2+}–PGA–Mn^{2+}GDP, and PEPCK–Mn^{2+}–oxalate–Mn^{2+}GTP complexes*

	PEPCK–Mn^{2+}–β-SP–Mn^{2+}GTP	PEPCK–Mn^{2+}–PGA–Mn^{2+}GDP	PEPCK–Mn^{2+}–oxalate-Mn^{2+}GTP (oxalate soaked)	PEPCK–Mn^{2+}–oxalate–Mn^{2+}GTP (cocrystal)
Wavelength, Å	0.9	0.9	0.9	0.9
Space group	$P2_1$	$P2_1$	$P2_1$	$P2_12_12_1$
Unit cell	$a = 62.0$ Å	$a = 62.2$ Å	$a = 60.5$ Å	$a = 60.4$ Å
	$b = 119.5$ Å	$b = 119.7$ Å	$b = 119.8$ Å	$b = 84.9$ Å
	$c = 87.3$ Å	$c = 86.8$ Å	$c = 87.3$ Å	$c = 119.0$ Å
	$\alpha = \gamma = 90.0°$	$\alpha = \gamma = 90°$	$\alpha = \gamma = 90°$	$\alpha = \beta = \gamma = 90°$
	$\beta = 107.1°$	$\beta = 107.1°$	$\beta = 96.7°$	
Resolution limits, Å	29.2–1.5	28.8–1.3	30.0–1.45	33.2–1.5
No. of unique reflections	178,266	276,410	206,173	93,846
Completeness†, % (all data)	97.3 (81.4)	97.7 (84.3)	99.8 (97.1)	99.8 (98.4)
Redundancy†	6.5	6.7	7.1	6.9
$I/\sigma_{(I)}$†	17.7 (1.7)	21.5(1.6)	21.9(2.2)	20.4 (2.5)
R_{merge}†‡	0.05 (0.59)	0.08 (0.57)	0.05 (0.51)	0.06 (0.60)
No. of ASU molecules	2	2	2	1
R_{free}†§ (%)	20.9 (34.9)	19.3 (34.3)	20.3 (30.7)	18.5 (27.1)
R_{work}†¶ (%)	17.6 (32.4)	16.9 (33.7)	17.5 (29.5)	16.0 (23.7)
Average *B* values‖				
Protein	Mol A = 8.32	Mol A = 9.69	Mol A = 10.17	9.20
	Mol B = 8.45	Mol B = 10.78	Mol B = 9.83	
Water	19.04	23.04	22.2	27.03
Ligands	β-SP	PGA	Oxalate	Oxalate
	Mol A = 5.72	Mol A = 5.82	Mol A = 10.02	7.99
	Mol B = 5.14	Mol B = 10.31	Mol B = 8.17	
	GTP	GDP	GTP	GTP
	Mol A = 4.57	Mol A = 4.77	Mol A = 6.88	7.47
	Mol B = 5.64	Mol B = 8.13	Mol B = 6.38	
Estimated coordinate error based on maximum likelihood, Å	0.05	0.03	0.05	0.04
Bond length rmsd, Å	0.019	0.013	0.016	0.011
Bond angle rmsd, °	1.72	1.51	1.65	1.40
Ramachandran statistics (preferred, allowed, outliers), %	96.4, 2.9, 0.7	96.9, 2.4, 0.7	96.7, 3.5, 0.8	96.2, 3.0, 0.8

*Mol A, molecule A of the crystallographic dimer; Mol B, molecule B of the crystallographic dimer.

†Values in parentheses represent statistics for data in the highest-resolution shells. The highest-resolution shell comprises data in the range of 1.55–1.50, 1.35–1.3, 1.50–1.45, and 1.55–1.50 for the PEPCK–Mn^{2+}–β-SP–Mn^{2+}GTP, PEPCK–Mn^{2+}–PGA–Mn^{2+}GDP, PEPCK–Mn^{2+}–oxalate–Mn^{2+}GTP (soaked), and PEPCK–Mn^{2+}–oxalate–Mn^{2+}GTP (cocrystal) datasets, respectively.

‡$R_{merge} = \Sigma\ |I_{obs} - I_{avg}|/\Sigma\ I_{obs}$.

§See Brunger (1) for a description of R_{free}.

¶$R_{work} = \Sigma||F_{obs}| - |F_{calc}||/\Sigma|F_{obs}|$.

‖*B* values indicated are residual *B* values after TLS refinement.

1. Brunger AT (1992) Free R-value: A novel statistical quantity for assessing the accuracy of crystal-structures. *Nature* 355:472–475.